OPEN ACCESS

Experimental Investigation of PEM Water Electrolyser Stack Performance Under Dynamic Operation Conditions

To cite this article: Jingjing Liu *et al* 2024 *J. Electrochem. Soc.* **171** 054521

Journal of The Electrochemical Society, 2024 **171** 054521

Experimental Investigation of PEM Water Electrolyser Stack Performance Under Dynamic Operation Conditions

Jingjing Liu,[1,z] Liuyi Huang,[1] Jérôme Leveneur,[2] Holger Fiedler,[3] Sam Clarke,[1] Thea Larsen,[4] John Kennedy,[3,5] and Mark Taylor[1]

[1]*University of Auckland, Department of Chemical and Materials Engineering, Auckland, 1023, New Zealand*
[2]*Bspkl, b.spkl Limited, Lower Hutt 5010, New Zealand*
[3]*National Isotope Centre, GNS Science, Lower Hutt 5010, New Zealand*
[4]*University of Auckland, Department of Electrical, Computer and Software Engineering, Auckland 1023, New Zealand*
[5]*The MacDiarmid Institute for Advanced Materials and Nanotechnology, Wellington 6140, New Zealand*

Water electrolysis has been used to produce green hydrogen, for which identifying optimum operation parameters is crucial to improve its energy efficiency and energy consumption. This paper used a commercial proton exchange membrane (PEM) water electrolyser stack (180 W) to demonstrate the correlation between operating current change, temperature, and water flow rate and their impact on the thermal and electrical performance of the stack. It was found that the current control regime and temperature control can offset the voltage ageing in a long-term operating electrolyser with no negative impact on the H_2 production rate. For a controlled decreasing current path, in the medium range of operating current, the stack's energy efficiency was improved by 5%, and 3.7% specific energy consumption can be saved comparing to the standard operation (57.8 $kWh{\cdot}kg^{-1}H_2$). The results provide insights into the potential optimisation in operation conditions to further increase cell energy efficiency and reduce energy consumption. This new finding sheds light on developing an energy- and cost-saving operating method for long-term green hydrogen production via water electrolysis.
 [DOI: 10.1149/1945-7111/ad4d1f]

Manuscript submitted January 7, 2024; revised manuscript received April 9, 2024. Published May 28, 2024.

Since 1671, when hydrogen (H_2) gas was first discovered and described as a product of the reaction between iron filings and dilute acid, it has grown into a key feedstock to many industries such as oil refineries, metallic ore reduction, ammonia and methanol production, sustainable fuels and decarbonising the hard-to-abate industries.[1] Green H_2, produced from zero-carbon emission resources and processes, will likely be a technology enabling the global energy transition from fossil fuel to sustainable energy. Water electrolysers, such as alkaline water electrolysers (AWE) and proton exchange membrane water electrolysers (PEMWE), are commercialised technologies for producing green H_2 using renewable energy-sourced electricity.[2,3] In a water electrolyser, the applied electrochemical potential drives the reaction of water splitting into H_2 and O_2 gases ($2H_2O \rightarrow 2H_2 + O_2$). Thus, abundant renewable energy can be stored seasonally in H_2 gas.[1,4,5]

The high cost of water electrolysers and relatively low energy conversion efficiency have historically hindered its wide deployment in industry[6–8] despite the high purity of H_2 produced. In an electrolyser stack, the materials used and primary design factors such as electrode area and the number of cells all play important roles in water electrolysis cell performance. However, these factors are not easy to change after commissioning an electrolyser system, hence the cell performance is operation-dependent once installed. The instability of the operation conditions should not be overlooked when intermittent renewable-energy-generated electricity is used to energise the electrolysis process.[9] Varying current density, mass and heat imbalance may penalise electrolyser lifespan and energy efficiency, especially for large-scale production facilities.[10–13] Understanding the response of a water electrolyser to dynamic conditions is critical to establishing efficient operation and control parameters for green H_2 production.

A power modulation will often be required to meet the power supply and/or product demand balance as in other large-scale electrolysis industries.[14,15] The frequency of current and voltage modification to an electrochemical system will interrupt the electrolysis process, and its impact for water electrolysis has been reported with controversial findings in the literature. Early reports of using pulsive directive current (DC) on AWE cells showed the possibility of enhancing its efficiency,[7,16–18] however that pulsive power input degraded the overall cell efficiency and gas purity as found later.[10–12] J. Koponen et al. applied pulsive current to AWE at controlled frequencies resonating with the dominant discharge component, showing maintained electrolysis cell performance.[19] Recent research showed with 3-dimensional electrodes (porous conductive anodes and cathodes) in AWE, higher energy efficiency was obtained when applying high voltage pulses together with optimum operating parameters.[20,21]

The PEMWE has recently become the leading contender technology for green H_2 production in the industry, owing to its high tolerance in wide current density range with high energy conversion efficiency compared to other electrolysers.[8,22–28] It's reported that rapid current ripple input to a PEMWE accelerates cell degradation, increasing cell resistance and mass transport limitation.[29,30] Aly H. Shaaban tested pulsed DC input with frequencies ranging from 10 Hz to 40 kHz, showing increased energy usage in a laboratory membrane water electrolyser.[31] In recent studies, the control systems[32,33] and high-frequency current ripples[34,35] were simulated in examining the dynamic response of a PEMWE stack to variable renewable electricity input, indicating that operation with favourable operating conditions are crucial in order to maximise the electrolyser efficiency and minimise the degradation. S. Boulevard et al. studied the voltage response to current density variation at a low values (0.04 to 0.96 $A{\cdot}cm^{-2}$) in a PEMWE, showing that a small step increase in current could cause voltage overshoot and a long time to stabilise the cell voltage.[30] A similar transient response in the stack voltage to current change was observed on a 1 kW PEMWE by R. García-Valverde, which however only analysed the thermal status.[36]

In contrast to the literature,[31] this research showed that a low frequency DC pulsation output into a PEMWE can increase the energy efficiency and reduce energy consumption in long term. Commercial PEM stacks were experimentally examined under various current variation paths and dynamic operation conditions including water flowrate and temperature. The outcomes revealed the dependence of the stack voltage, energy efficiency, and energy consumption on the controlled current pulsation and temperature.

[z]E-mail: jingjing.liu@auckland.ac.nz

Energy Requirement for Water Electrolysis

Electrochemical reaction.—In a typical structure of a PEMWE, the solid acidic membrane acts as the electrolyte, conducting H^+ proton from the anode to the cathode. Current is the controlled electrical energy input through electrodes and the electrochemical reaction takes place when the thermodynamic energy is met, separating H_2O into O_2 and H_2 gases as shown below:

$$H_2O\ (l) \rightarrow H_2(g) + \frac{1}{2}O_2(g)$$

$$\textit{Anodic reaction}: \quad H_2O \rightarrow \frac{1}{2}O_2 + 2H^+ + 2e^-$$

$$\textit{Cathodic reaction}: \quad 2H^+ + 2e^- \rightarrow H_2$$

Under standard conditions, the minimum amount of electricity (ΔG, Gibbs free energy) required at constant temperature and pressure for the decomposition of water is 237.2 kJ·mol^{-1}, and the standard enthalpy change of the reaction $\Delta H_d^\circ(H_2O(l))$, is 285.8 kJ·mol^{-1}. The standard reversible cell voltage E_{rev}° and thermo-neutral voltage E_{th}° for water splitting reaction to occur thus can be calculated as following:

$$E_{rev}^\circ = \frac{\Delta G_d^\circ(H_2O(l))}{2F} = 1.23\ V$$

$$E_{th}^\circ = \frac{\Delta H_d^\circ(H_2O(l))}{2F} = 1.48\ V$$

Kinetic energy is required to drive the reaction forward in addition to thermodynamic energy, resulting in higher cell voltage U_{cell} as shown below. Above E_{th}°, activation overpotential (η_{act}), ohmic resistance over potential (η_{ohm}) and mass transfer overpotential (η_{trans}), and overpotential induced by bubble when it applies, are required.

$$U_{cell} = E + \eta_{act} + \eta_{ohm} + \eta_{trans} + \eta_{bubble}$$

The reversible cell voltage can be determined from the Nernst equation, and is a function of temperature as below:[8,22,37]

$$E = E^\circ + \frac{RT}{nF}\ln\left(\frac{P_{H_2} \cdot P_{O_2}^{\frac{1}{2}}}{\alpha_{H_2O}}\right) = \frac{\Delta_r H^\circ - T\Delta_r S^\circ}{nF} + \frac{RT}{nF}\ln\left(P_{H_2} \cdot P_{O_2}^{\frac{1}{2}}\right)$$

Activation overpotential η_{act} is given below, and it follows that at higher temperatures, the overvoltage applied is reduced:[37–41]

$$\eta_{act} = \frac{\Delta G^\ddagger}{\alpha F} - \frac{RT}{\alpha F}\ln\left(\frac{F\ c\ k_B T}{j\ h}\right)$$

Ohmic overpotential η_{ohm} refers to the voltage drop due to electrical resistance from cell components.[22] It can be split into the resistance due to electrically conducting components, and the resistance due to the cell membrane, which conducts protons.[22] At higher temperatures, the resistance of metallic conductors increases.[42] However, in PEM electrolysis cells the resistance of oxide layers and the cell membrane are much more significant,[36,43] and their resistance decreases at higher temperatures.[22,36] Therefore, we would expect ohmic overpotential to decrease at higher temperatures.

$$\eta_{ohm} = R_{cell}I + \frac{\delta_{mem}}{A\ \sigma_{mem}}\ I$$

where $\sigma_{mem} = (0.005139\lambda - 0.00326)\exp\left[1268\ \left(\frac{1}{303} - \frac{1}{T_{mem}}\right)\right]$

In order for the electrolysis reaction to take place, reactants must diffuse to their respective electrodes. At higher current densities, electrolysis may become mass transport limited.[36,38] The effect of diffusion on overpotential η_{trans} at steady state can be described using a combination of Fick's first law and the Nernst equation:[22]

$$J = -D_{eff}\left(\frac{\partial c_i}{\partial x}\right)$$

$$\eta_{trans,an} = \frac{RT_{an}}{nF}\ln\frac{C_{O_2,mem}}{C_{O_2,mem,0}}$$

$$\eta_{trans,cat} = \frac{RT_{cat}}{nF}\ln\frac{C_{H_2,mem}}{C_{H_2,mem,0}}$$

Where J is the diffusion flux in the x direction, D_{eff} is the effective diffusivity of the medium species are transported in, and C_i is the concentration of species i. Diffusion is assumed to occur in only one dimension. $C_{i,mem}$ is the concentration of species i at the interface between the membrane and the electrode, and $C_{i,mem,0}$ is the concentration at a reference condition. The diffusion overpotential is not directly affected by temperature, but the diffusivity may increase, and diffusion overpotential can also be affected by the bubble mobility and overpotential.

In practice, electrolysers are often operated at high current density (above 1 A·cm^{-2}). The subsequent increase of overpotentials leads to higher energy loss. Typical cell voltages are reported within the range of 1.8 to 2.1 V,[8,44] therefore having up to 40% energy loss when converting electrical energy to the electrochemical energy. This low energy conversion rate or efficiency from electricity to hydrogen has been one of the contributors to the high cost of green H_2 production. Improving energy efficiency while increasing productivity (current density) has been a challenge to many industrial electrolysis processes,

Energy efficiency and energy consumption.—The energy conversion efficiency of a water electrolyser indicates if the device has adequate energy consumption to producing the hydrogen using electricity. Energy efficiency and total energy consumption (Energy = $\text{Volts}_{\text{stack}}$ × electrical current) per unit of mass of H_2 produced (referred as specific energy consumption in kWh·kg^{-1} or kWh·Nm^{-3}) have been widely used to evaluate the electrolyser energy performance.[45] For a large-scale industrial electrolyser stack, a high H_2 production rate (e.g. high current densities) can potentially reduce the energy consumption and capital cost per kg H_2 generated. High current densities also improve energy storage capacity when surplus and intermittent renewable energies are available.

Lamy and Millet[8] reviewed different methods in calculating energy efficiency. From a fundamental perspective, energy efficiency is the ratio of the minimum amount of energy splitting one mole of H_2O under reversible conditions to the total energy consumed under irreversible conditions. Energy efficiency correlates cell voltage at standard conditions (25 °C, 1 atm, liquid water) and can be simplified as shown below:

$$\varepsilon_{energy} = \frac{\Delta H_{rev}}{\Delta H_{rev} + nF\eta_{loss}} = \frac{E_{th}}{E_{th} + E - E_{rev}} = \frac{1.48}{0.25 + U_{cell}}$$

It is reported that the energy efficiency of a PEMWE can be up to 80%–85% in the laboratory,[6] however further loss in efficiency will occur at a stack scale, hence increase in energy consumption.

Maintaining the energy efficiency may be even more challenging under dynamic operations due to the intermittent nature of renewable energy when these cells are scaled up for industrial production[46–50] or the need for high/low hydrogen throughput leading to variable current density.[51]

Experimental Method

Water electrolysis system.—In this research, two PEMWE stacks (QLC-500 Model and 60Z series Nafion 117, see Table I) were tested in a water electrolysis system, as shown in Fig. 1a, consisting of water and gas circulation, power supply and data acquisition. A data logger recorded the stack and water temperatures, current and voltage data in real time, and H_2 flowrate was monitored using a volumetric flowmeter. Results obtained from QLC-500 Model 2-cell stack, also validated in 60Z series, are used in this paper.

Operation parameters.— *Power.*—The PEMWE was powered by a DC power controller (Hewlett Packard model 6672 A). DC input was regulated for different power control regime in terms of frequency and increase/decrease step change of operating current. Voltage was recorded as output.

Water and temperature.—A peristaltic pump circulated distilled water through the electrolyser stack and system, then back to the 5 L water reservoir. A thermal water bath controlled the inlet water temperature before entering the stack. Three thermocouples were installed at different locations (see Fig. 1a) to monitor the system temperature:

T1–water bath temperature, ambient or heated to around 60 °C.

T2–water inlet temperature, temperature of the water that was fed to the electrolyser.

T3–water outlet temperature, temperature of the water at the vicinity of the anode before exit the water electrolyser.

There was no possibility to maintain the same water temperature across the system and between the water inlet and outlet of the commercial electrolyser stack, which was also reported in literature.[36] There was about 10 °C drop in 30 cm flow distance from the water bath to electrolyser inlet. Under a constant water flow rate, the temperature increase between the water inlet and outlet across the QLC-500 2 cell Stack was 20 °C ∼ 40 °C due to the joule heating caused by the operating current.

H_2 gas.—The system gas pressure was at standard condition with no pressure regulation. H_2 gas coming out of the cathode was dried by a water trap and a gas dryer unit respectively to remove the saturated moisture. H_2 gas flow rate was then measured by a H_2 volumetric flowmeter. The H_2 output showed a first order fluctuation during the transient state after tuning the current; therefore, H_2 flowrate reading were only recorded once it stabilised at steady state within approximate 15 mins.

Results and Discussion

The electrolyser stack performance was tested under controlled parameters of water temperature, water flowrate, and low frequency step changing DC input. Energy efficiency and energy consumption were calculated from the measured voltage and current. Both electrolysers showed repeated energy efficiency improvement trend when applying low frequency step changing DC. Only data obtained from QLC-500 Model Stack are used and discussed in this paper. Note that the stack voltage recorded in this paper thus represents the voltage of two cells connecting in series. To reflect the actual control parameter in current in the experiments, this paper uses current instead of current density. To convert the value of current to current density, refer to Table I.

Table I. Water electrolyser stack technical data.

	QLC-500 model stack	60Z series stack
Active Area	56 cm^2	1.247 cm^2
Stack Size	2	1
Operating Current Range	0–36 A	0−9 A
Max Current Density	0.536 A cm^{-2}	7.217 A cm^{-2}
Voltage Range	2.2–5 V	1.45–2.2 V
Manufacturer	Shandong Saikesaisi Energy Company	Fuel cell store

Behaviour of the PEMWE under dynamic operation modes.— The interrelation between dynamic conditions in **water flowrate**, **step changes in current** and **water temperature** were tested, see Table II, to investigate their impact on the stack voltage and energy performance.

Water flowrate control.—Constant water flow rates, 32 ml·min^{-1} and 223 ml·min^{-1} were used, respectively, during the operation of the water electrolyser, as shown in Fig. 2. The operating electric current increased directly from 0 A to the operating value for each run, i.e. 0 → 5 A, 0 → 10 A, 0 → 15 A, 0 → 20 A, 0 → 25 A, 0 → 30 A, and 0 → 36 A. The stack cooled down to room temperature after each run to ensure the same initial thermal state of the electrolyser stack.

As shown in Fig. 2b-1, with a constant water flowrate of 32 ml·min^{-1} the electrolyser temperature and voltage showed an incremental increase following the operating current increase and reached steady states within 30 mins. The temperature difference between the start-up and steady state varied between 1 °C to 20 °C across the operating current 5 A to 36 A. This steady state was defined as the ***Absolute Steady State (ASS)*** as a reference point for comparison later. A higher water flowrate 223 ml·min^{-1} significantly reduced the cell temperature for current above 15 A, and at lower current the temperature didn't show a similar increase with current as the low water flowrate 32 ml·min^{-1}. For current above 15 A, the cell voltages were independent of the current increase and converged at higher values, as shown in Fig. 2b-2.

These results suggest that water flowrate plays a critical role in thermal balance management of the water electrolyser stack. Overall, higher water flow mitigated temperature variation comparing to the low water flowrate across the whole operating range of 5 A to 36 A. With high-water flowrate, the stack temperature was lowered due to the consequent high heat transfer coefficient (and lower water temperature rise) between the water and stack, hence high heat removal. Enhanced heat dissipation from the stack to water flow shifted the heat balance down, i.e. lower thermal status, thus resulting in cell voltage rise due to increased overpotentials. Mass transfer could be improved due to faster bubble removal as well as by the high-water flow; however, although the bubble overpotential could be decreased with high diffusion rate of species at the electrode interface, the significant voltage increase induced by stack temperature drop was greater. It is reasonable to conclude from the observed results that the impact of high-water flow on thermal balance (thus voltage) overtook the improved mass transport. With higher water flowrate, the drawback is therefore not unexpected as a consequent higher cell voltage at steady state, as observed in this research, energy efficiency loss was therefore higher, as was energy consumption.

Impact of step-changing current operating paths.—Low water flowrate of 32 ml H_2O·min^{-1} was used in the following experiments with step changing in current with an interval of 5 A. A PEMWE stack behaviour anomaly was identified. When approaching the same operating current via different paths, stepping up or stepping down, its endpoint voltage and temperature stabilised (within 30 mins) at different levels. As shown in Figs. 3a-1 and 3b-1, the steady state endpoint voltage in *decreasing current path* were much lower than

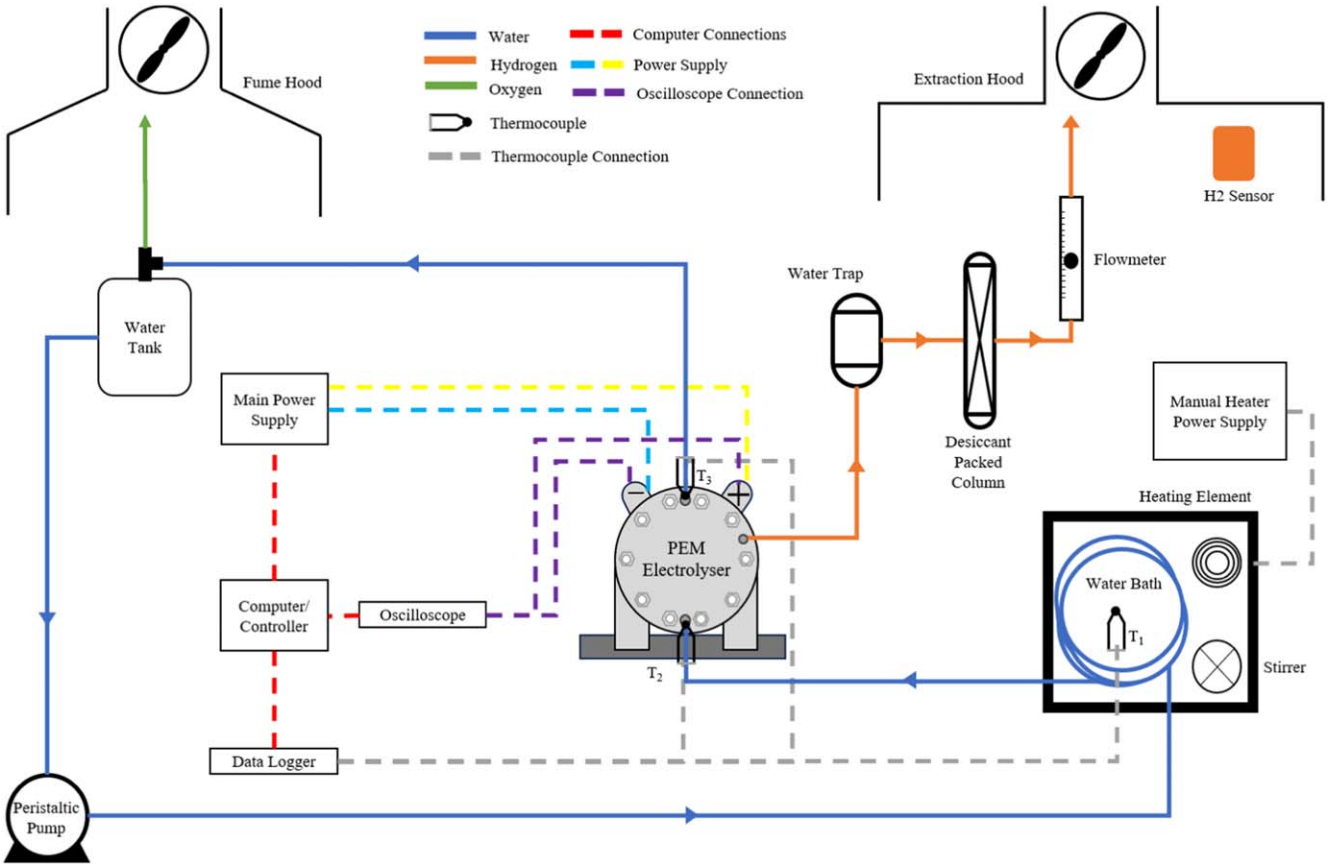

Figure 1. A water electrolysis system.

increasing current path in the middle range current (10–30 A), up to 21%. Hence efficiency gain for decreasing current step change current below 30 A. This phenomenon repeated across the whole lifespan of two electrolyser stacks as tested, and higher efficiency gain at the later stage of the electrolyser stack operation was observed.

The water temperatures measured were a linear function of current change, which suggested that the internal ohmic heating caused the thermal status change of the electrolyser following stepwise ascending current. However, the temperature increase of the electrolyser in this case didn't benefit the stack voltage reduction when compared to the descending current path. This was contrary to the temperature-controlled experimental results in the literature, which state that cell overpotentials reduced with higher cell temperature.[52,53] As shown in Figs. 3a-2 and 3b-2, although the resulting stack temperature following the *increasing current* step change was 5 °C–8 °C higher than *decreasing current step change path*; yet, stack voltages were markedly higher. The root cause of the stack behaviour anomaly will be explored in a simplified heat balance model later in this paper, which will be further explained in kinetic and computation models in a separate paper.

To the best of the authors' knowledge, this phenomenon of voltage change under stepwise current change has never been reported. Althoug this is not a conventional cell operating conditions, it is important to raise awareness in thermal management to the water electrolyser community for a safer and more effective control when operating at a large stack scale with intermittent power supply and/or varying current densites.

Impact of water temperature variation.—Significant cell voltage aging was observed after 24 months intermittent operation although the repeatability of the cell voltage improved. As shown in Fig. 4a, the voltage - current curve taken in 2023 has shifted significantly left and up, i.e. the sharp increase of voltage at low current then began to taper off comparing to initial run in 2020. Speaking in efficiency terms, this means that for the same production of hydrogen at the same current value a much greater amount of voltage is required. It in turn translates to a greater power requirement ($P = VI$) and lower overall electrolyser efficiency.

The electrolyser was operated at two temperatures in 2023 to examine effect of controlled water bath temperature on the cell voltage - ambient temperature vs temperature-controlled (60 °C). Note that for the latter, at high operating current (above 20 A), the water flowrate had to increase accordingly to maintain the stack temperature under safe operating range (below 70 °C) to counteract the joule heating effect within the cell stack.

Higher inlet water bath temperature (60 °C) no doubt increased the cell efficiency by a downshifting in the voltage required, see Fig. 4b. From our data it is reasonable to suggest that as water inlet temperature increased the voltage drawn decreased at high current. These IV curves agreed with the previous research[52,53] that increase in water temperature reduces the efficiency loss of the PEM electrolyser, due to the reduced energy requirements to split the water molecules. However, energy for heating up the water temperature can outweigh the reduced power required by the cell, especially at the start up stage. Deploying an intermittent power supply can raise the complexity of the stack thermal management with high inlet water temperature.

Temperature control plus current step change.—A $15 \rightarrow 20 \rightarrow 25 \rightarrow 20 \rightarrow 15$ A step changing current was tested under both ambient and high temperature (water bath 60 °C) conditions in 2023. In both runs, the water electrolyser temperature increased with the operating electric current. For the high water temperature run (60 °C), the pump speed had to be turned up to maintain the stack temperature within the safe thermal operation range for high

Table II. Experimental design of different operation dynamic conditions with current step change.

Operating current step change	Water flow rate	Start-up water inlet temperature	Highest water outlet temperature	Current step change/A
i - Off/On to the endpoint current steady state	32 ml·min^{-1} (**Absolute steady state** as a baseline for comparison)	Ambient (23 °C)	44 °C at 36 A	0 → 5, 0 → 10, 0 → 15, 0 → 20, 0 → 25, 0 → 30, 0 → 36
	223 ml·min^{-1}	Ambient (23 °C)	31 °C at 36 A	
ii - Incrementally increasing current	32 ml·min^{-1}	Ambient (22 °C)	48 °C at 36 A	0 → 5 → 10 → 15 → 20 → 25 → 30 → 36
iii - Incrementally decreasing current		Ambient (23 °C)	44 °C at 36 A	0 → 36 → 30 → 25 → 20 → 15 → 10 → 5
iv - Incrementally increasing, then decreasing current	80 ml·mil^{-1}	Controlled water temperature (44 °C)	55 °C at 25 A	0 → 15 → 20 → 25 → 20 → 15 A
	Increased pump speed to maintain the temperature-controlled experiment at a safe operating temperature	(Cooling down from 60°C water bath)		
		Ambient (21 °C)	25 °C at 25 A	

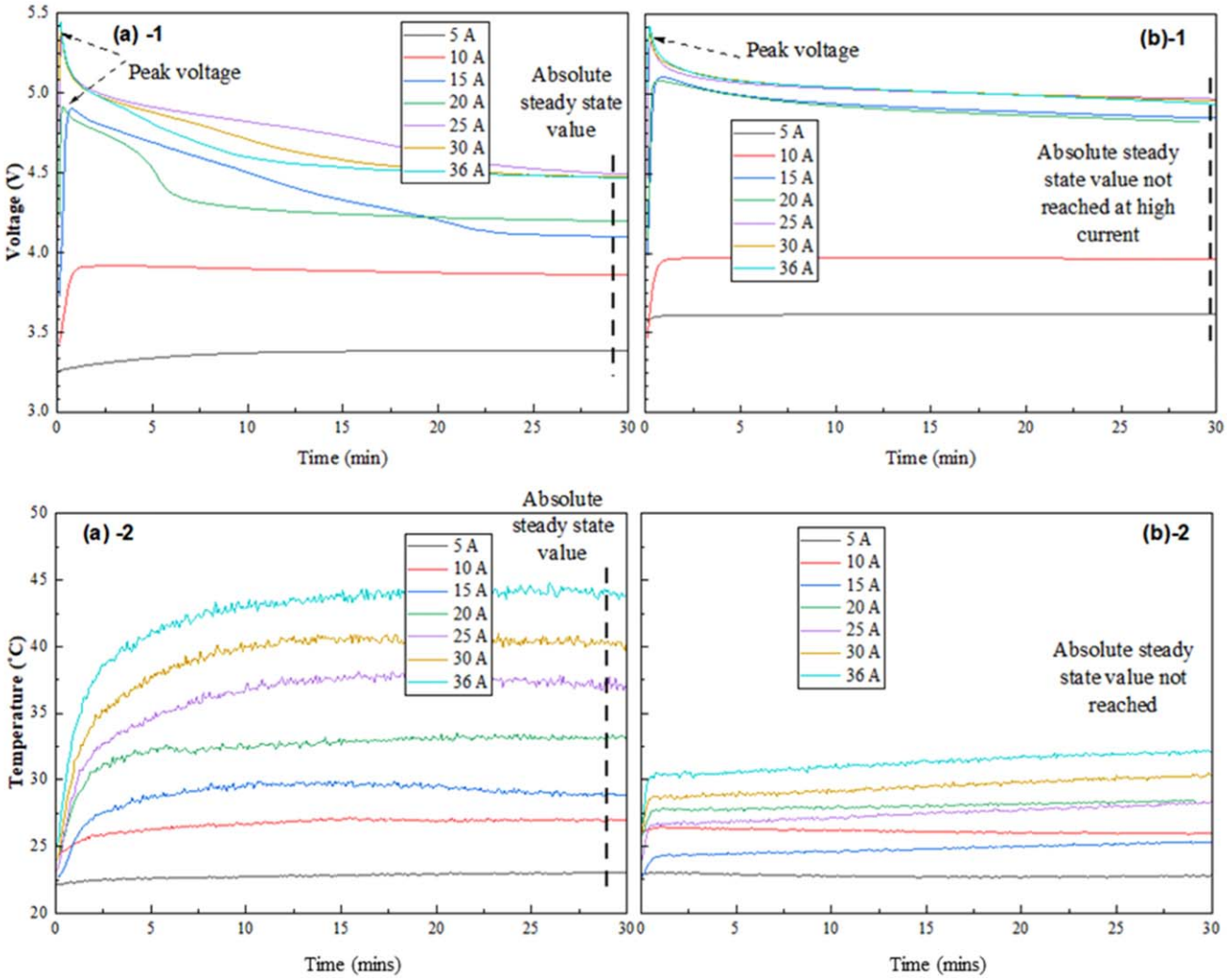

Figure 2. Voltage and Temperature profiles with different water flowrate: (a) 32 ml $H_2O \cdot min^{-1}$ and (b) 223 ml $H_2O \cdot min^{-1}$.

current (>20 A). It was observed that in addition to lower voltage for the duration of the experiment, the high temperature experiment had a higher voltage drop of ~8% at 15 A compared to the max drop of the ambient temperature experiment being ~4%, as shown in Fig. 5a. No significant discrepancy in hydrogen production rate was observed between the ambient and high temperature experiments, and before and after the overshoot, see Fig. 5b. The variability of hydrogen flowrate was within the fluctuation range as observed in all the experiments.

Heat balance model.—A heat balance model is proposed to describe the inconsistent impact of temperature on the cell voltage under dynamic operations. As shown in Fig. 6, the total energy input to the electrolyser is the electric power supplied, $Q = I \cdot U_{cell}$. U_{cell} is composed of the electrochemical potential equivalent to the endothermic electrochemical reaction of water splitting E_{React}, the overpotentials for activation (η_{act}), ohmic resistance (η_{ohm}) and mass transfer (η_{trans}) and η_{bubble}. Overpotentials are dependent on temperature during the operation as discussed in 2.1 Electrochemical reaction.

After the endothermic electrolysis water splitting to H_2 and O_2 ($I \cdot E_{React}$), the surplus energy ($Q_{surplus}$) remains from the total energy input and is released as heat. The surplus heat energy is then dissipated (Q_{Diss}), from the electrochemical reaction zone to water across the heat flux boundary, i.e. the water and solid electrodes interface; then the surplus heat is removed by water flow (Q_{Wat}). The instantaneous balance between the Q_{Diss} and Q_{Wat} is determined by equilibrium between the internal joule heating and the external water temperature. The heat transfer balance is shifted up/down following the varied cell conditions and thermal status, resulting in a possible hysteresis in the corresponding cell voltage as follows below.

At steady state, the heat transfer across the boundary is balanced as below:

$$Q_{Diss} = Q_{Wat}$$

$$Q_{Diss} = I\ U_{cell} - I\ E_{React}$$

$$Q_{Wat} = m\ C_{p,water}(T_{Wat} - T_{initial}) = h\ (T_{interface} - T_{Wat})$$

Under above three dynamic operation conditions (water flowrate, current increasing/decreasing path, and water temperature) investigated in this research, the variation in water flowrate, temperature and current introduced instantaneous imbalances in the heat flow, see Table III. Within the electrolyser, the heat transfer direction is based on the temperature difference between two phase interface boundaries - $T_{interface}$ and T_{wat}, and the heat transfer coefficient h (determined by water flowrate). With heat flux flowing from water to reserved surplus heat energy, the external energy supplied to the electrochemical energy lowers the heat dissipation, hence lowers cell voltage. Vice versa, when the heat dissipated from the surplus energy becomes greater, the corresponding voltage is growing higher.

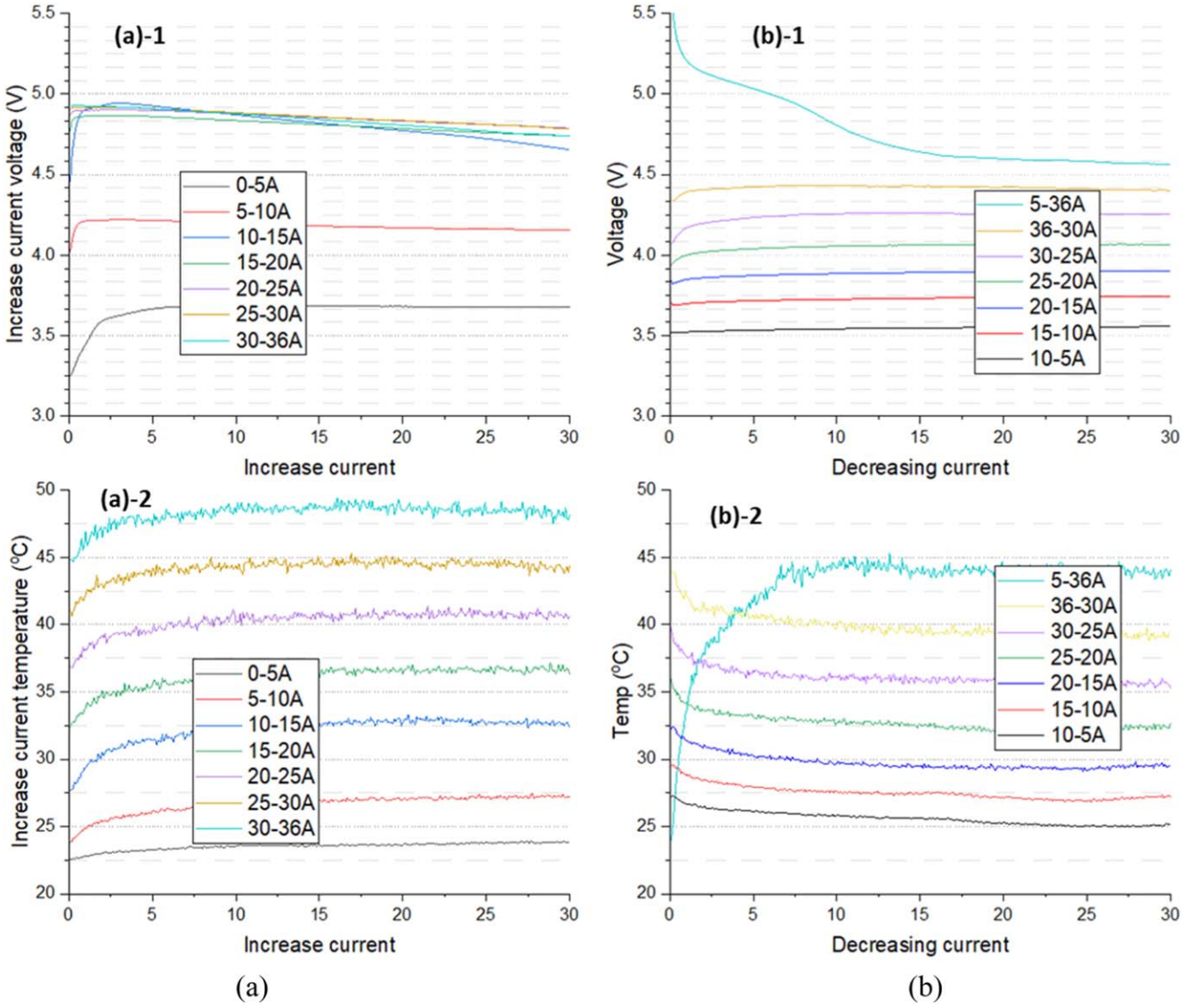

Figure 3. Comparison of voltage and temperature profile under different operation modes: (a) increasing current step change; (b) decreasing current step change.

Voltage instability over life span.—A trending voltage decay of the electrolyser stack was investigated across the whole life span from 2021 to 2023, mainly at the low current density range. For higher current density range, the voltage converged at a plateau regardless the increase of the current. At early life stage for the first 12 months as shown in Fig. 7, instability of the voltage was observed. Improved repeatability was only observed when operating at the later life within short period of shutdown, see Fig. 5.

The electrolyser stack voltage-current was characterised by alternating the current ramping up rates from 0 to 36 A with constant water flowrate as shown in Fig. 7. In the named ***I-V curves 1 & 2***, the current was tuned up with a step increase of 0.03 A–0.6 A within a minute, the immediate cell voltage after turning up the current was recorded. For a ***Slow-Scan***, the current increased with an interval of 1 A every 5 mins and the voltage was recorded before turning up the current. ***Steady-State*** voltages were recorded after the stack reached electrical and thermal balances in about 30 min, with a current step increase of 2 A.

The electrolyser showed wide variability in voltage when operating at different current increasing frequency, which might be attributed to the instability of voltage after current increase as well as not reaching the steady state in a limited holding time. At steady states, early life stack voltage was within the variability with different ramping up rate in current while a long term shut down period caused significant voltage ageing which was also observed by S. Boulevard[30] after a 15-day shutdown. Voltage increased further with longer operation hours. However, the measured H_2 production at steady state showed good repeatability across the whole lifespan, see Figs. 7b and 5b.

Across the whole testing current regime, the stack voltage plateaued when the operating current was above approximately 25 A. This plateau was also observed by Á. Hernández-Gómez et al. in a static voltage-current curve of a commercial 400 W PEMWE.[34] With a constant water flow rate, stack temperature increased following the current input increase. We hypothesize that the voltage increase might be hindered due to the temperature increase at high current densities.[54] Although bubble formation can increase the overpotentials at high current densities,[55–57] the significant difference in the magnitude between electric conductivity and ionic conductivity due to the stack temperature increase results in lower overall ohmic resistance, therefore offsetting the voltage increase.[58]

An unplanned power cut during the measurement of *I-V curve 2* escalated the voltage discrepancy, see in Fig. 7a. Although the stack was switched on immediately back to 23 A, the stack voltage remained lower than before the power cut until it plateaued at the current 36 A.

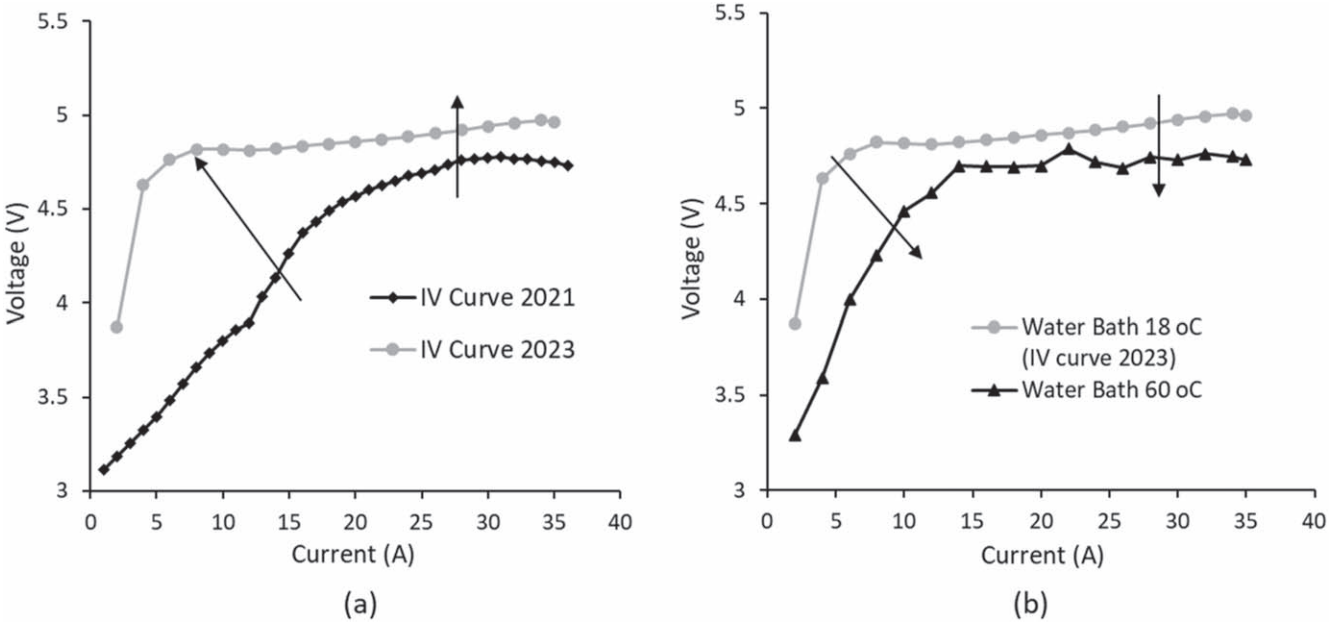

Figure 4. (a) IV curve of new and degraded electrolyser; (b) IV curve of high and low temperature operation.

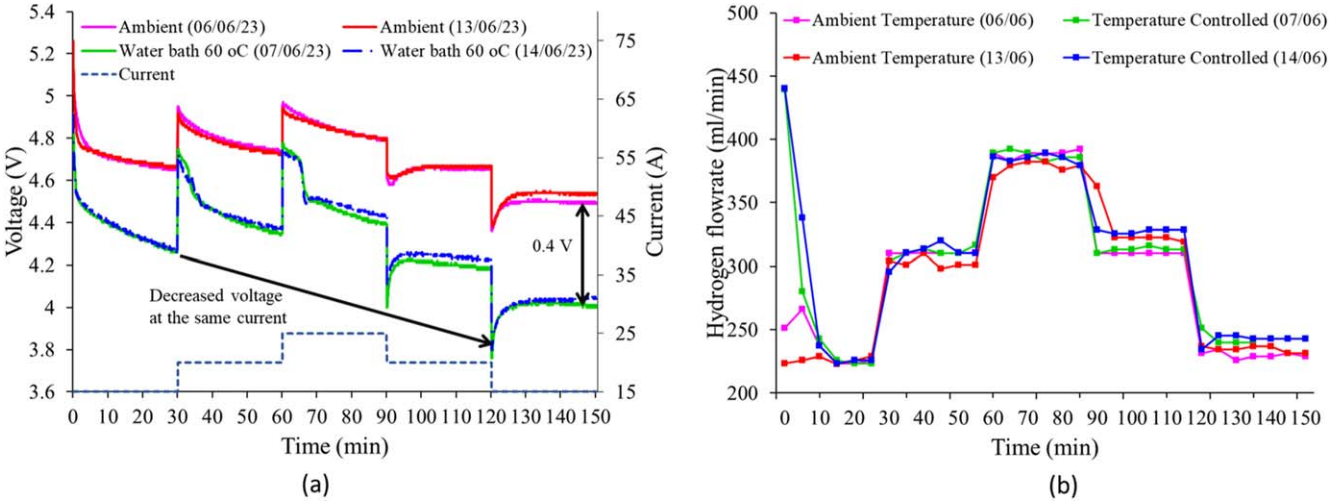

Figure 5. With a 15 → 20 → 25 → 20 → 15 A step changing current route (a) Stack voltage comparison between ambient temperature and controlled temperature 60 °C; (b) Measured hydrogen flowrate for each run.

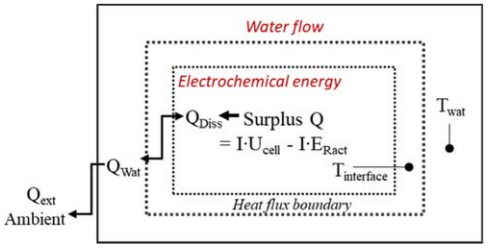

Figure 6. A simplified heat transfer balance model within the water electrolyser stack.

Energy performance analysis.— *Energy efficiency.*—Cell voltage and current input are the key factors to determine the electrolyser energy efficiency. Lower cell voltage is equivelant to higher energy efficiency. *Current* and *Temperature* are widely recognised as key parameters that affect cell voltage, hence improving the energy efficiency, which was examined in this research. The impact of *operating current step change* on energy efficiency was also firsly studied in this paper.

Current and temperature.—As shown in Fig. 8a, the electrolyser stack energy efficiency decreased significantly from 2021 to 2023, following the voltage aging. This decrease was particularly evident at low current below 20 A. At 2 A and 4 A, there was a 12.6% and 18.1% reduction in efficiency, respectively. However, at high currents such as 30 A and 32 A, this efficiency loss was only in the region of a 1.7% to 2.2%. Therefore, it is reasonable to conclude that **electrolyser degradation more significantly affects efficiency reductions at low currents than high current operation**. Increasing water temperature (2023 run with 60 °C) as shown in Fig. 8b proved to be able to offset the efficiency loss due to the operation longevity. The efficiency was almost recovered to the same level with the 2021 electrolyser efficiency for current above 15 A. However, the low current performance (below 10 A) was still significantly degraded compared to 2021.

Table III. Voltage response to heat transfer direction under dynamic operating.

Dynamic operating	Q_{wat}	Heat flux transfer direction	Q_{Diss}	Voltage at new steady state
High water flowrate	Q_{wat} increase due to high HTC	←	Q_{Diss} increase following Q_{wat}	Higher voltage
Current ascending	Q_{wat} increase due to Higher $T_{interface}$ following Q_{Diss}	←	Q_{Diss} increase with current	Higher voltage
Current descending	Q_{wat} decrease due to lower $T_{interface}$ following Q_{Diss}	→	**Q_{Diss} decrease** with current	**Lower voltage**
High water temperature	Q_{wat} decrease due to higher T_{wat}	→	**Q_{Diss} decrease** following Q_{wat}	**Lower voltage**

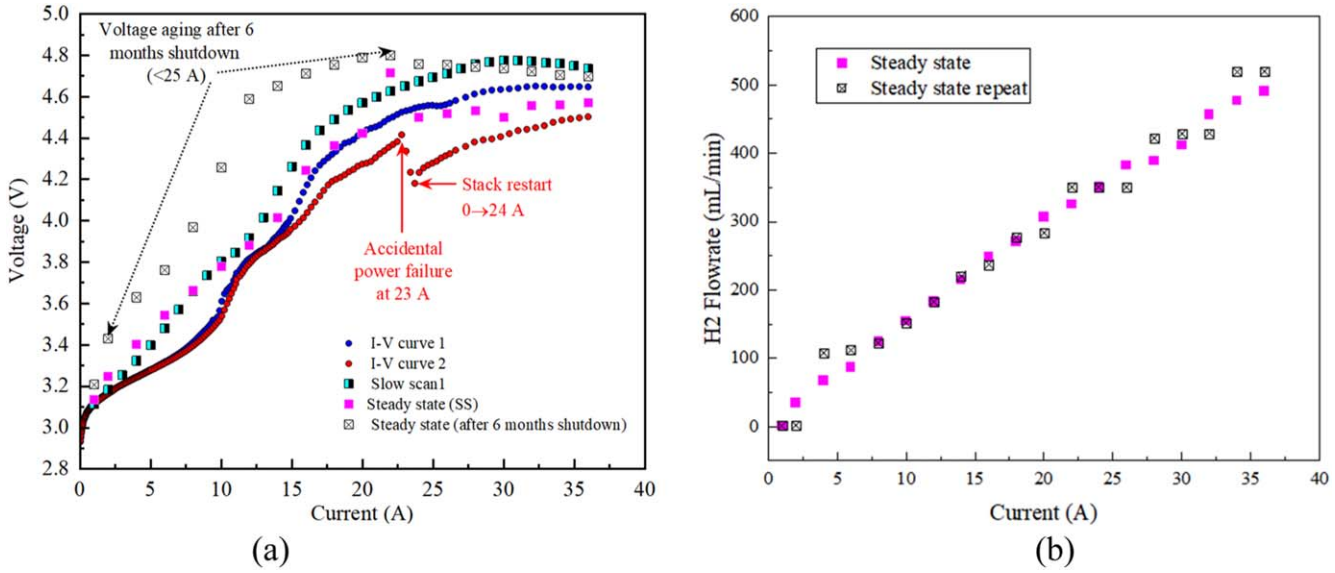

Figure 7. (a) Stack voltage under different frequency of step changing DC input, (b) H_2 production flowrate measured at steady state.

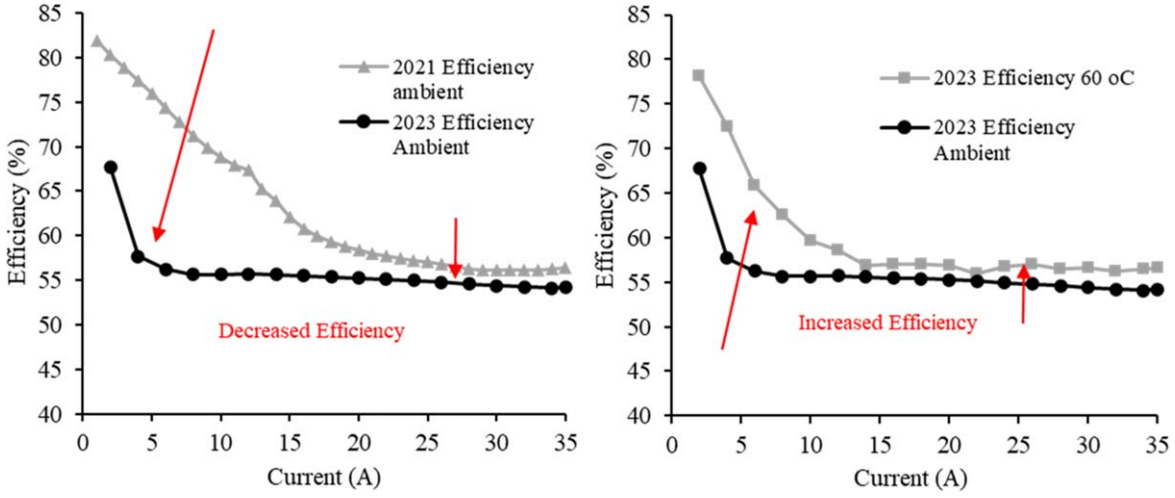

Figure 8. Comparison of Efficiency Curves measured at steady state for each current (a) 2021 vs 2023, (b) 18 °C vs 60 °C.

Operating current step change.—As shown in Fig. 9a, energy efficiency varied significantly for different current operating paths measured in 2021. The decreasing current path following the ***ASS*** showed an almost linear reduction in energy efficiency from 5 A to 36 A, while for the increasing current paths (*SSS* and *Increase current*) energy efficiency stayed lower across the whole current range, and plateaued after a sharp drop at the medium current (>15 A).

Energy consumption.—The total energy consumption for each operating current step change path was summed over the 30 mins operation period. The difference between the controlled current step-change paths and ***ASS*** was used to quantify the energy-saving scenario, as shown in Fig. 9b. The *decreasing current step-change path* reduced energy consumption for the medium current range (10 A–25 A), while *the increasing current step-change path* was negative (consumed more energy) for the whole operating current range (5 A–36 A).

The *increasing current step-change path* had the highest energy consumption, an extra 5.85 $kWh{\cdot}kg^{-1}$ H_2 compared to the ***ASS***. The *decreasing current step-change path* reduced energy consumption substantially (compared to ***ASS***), equivalent to 1.9 Wh within the total 3 h period. During the 3 h, the produced hydrogen is 3.9 g (from Faraday's law and assuming a 100% faradaic efficiency); thus, 0.5 $kWh{\cdot}kg^{-1}H_2$ energy was saved in the *decreasing current path* from the ***ASS*** energy consumption of 57.8 $kWh{\cdot}kg^{-1}H_2$. For the medium range of operating current (10 A-30 A) of *decreasing current path*, maximum 2.16 $kWh{\cdot}kg^{-1}H_2$ energy can be saved from the ASS energy consumption of 57.8 $kWh{\cdot}kg^{-1}H_2$.

A typical industrial-specific energy consumption of PEM water electrolysis was 58 $kWh{\cdot}kg^{-1}$ H_2, as reported for a 1.2 MW stack.[59] The PEM stack used in this research (57.8 $kWh{\cdot}kg^{-1}H_2$) is at a similar level of energy consumption to the 1.2 MW industrial PEMWE stack. Suppose a similar operation mode within the optimum current range was applied to this 1.2 MW industrial scale. The specific energy consumption could be reduced up to 2.17 $kWh{\cdot}kg^{-1}$ H_2, saving 44.9 kW power for a 1.2 MW stack. The power saving grows with the size of the electrolyser stack.

Materials degradation.—Over the operation period from 2021 to 2023, the QLC-500 Model Stack showed a significant decrease in efficiency, following a considerable voltage decay. Based on this voltage decay and the understanding of factors which contribute to cell voltage, we can suggest there has been a net increase in reversible potential and/or overpotentials. An autopsy of the

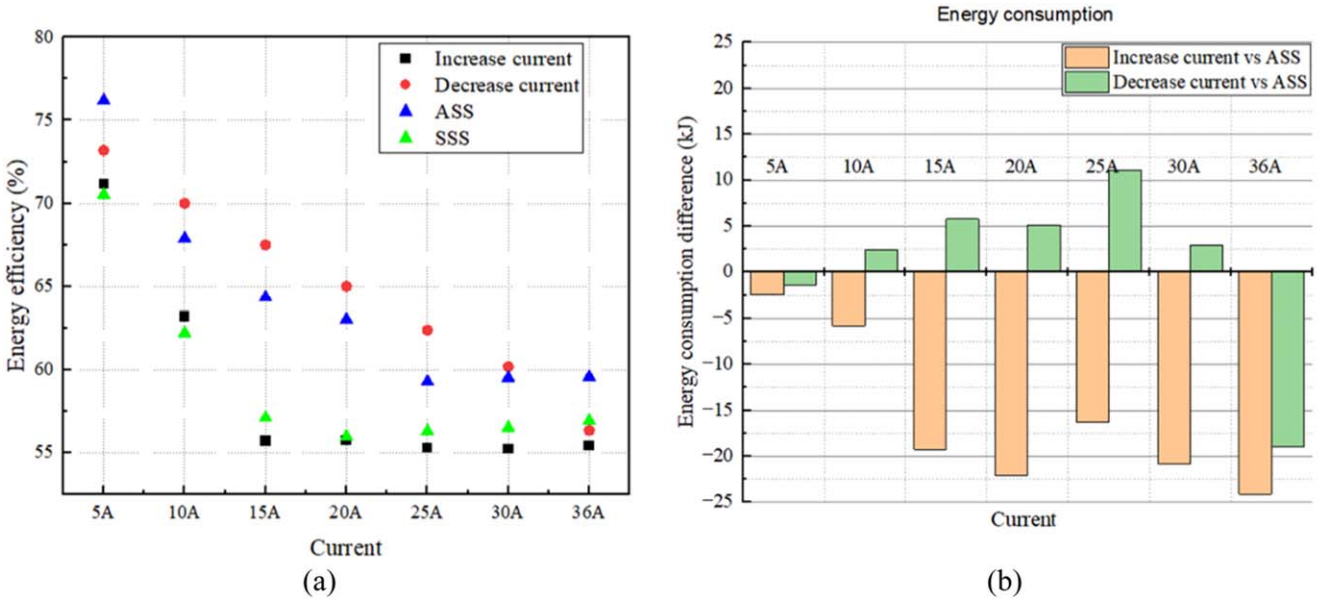

Figure 9. Electrolyser stack energy condition in 2021: (a) Energy efficiency at stabilised status under different operation routes. ASS- absolute steady state increase current from 0 to operating value; SSS- steady state with an incremental 2 A increase; Increase/decrease current with an interval of 5 A. (b) energy consumption saving between the *ASS* condition and increase/decrease operating current paths.

electrolyser indicated minor material wearing across the whole electrolyser, including MEA, GDL, BPP. The main contributor could be the passivation of the metal components, such as GDL and BPP, and wearing of catalyst layer. Further analysis of the materials by XRD, SEM and EDS have been taken and will be present in another paper.

Conclusions

This paper investigated the performance of PEMWE stacks under dynamic operation conditions, including water flowrate, temperature, and regulated step-change current input. The stack voltage, energy efficiency, and energy consumption were measured and compared. The following findings will provide insights in improving water electrolyser's operating energy efficiency:

- Water electrolyser voltage decays over operation longevity especially at low current density, hence the energy efficiency loss and driving up the cost and energy consumption per kg H_2 produced. This energy efficiency loss can be offset by careful thermal management of the electrolyser such as regulating the inlet water temperature and flowrate. Thermal management of the electrolyser can be complicated especially for large scale electrolyser stack due to the joule heating effect when increasing the operating current density. The associated stack temperature increase due to joule heating doesn't lower the stack voltage in this case.
- Compared to a traditional constant DC supply, a step changing current control regime should be considered in improving the operating energy efficiency. A step up (increasing) in the current input is proved to depress stack efficiency and increase energy consumption, while step down in current appears to improve stack efficiency and reduce energy consumption. This effect can be enhanced with careful thermal management of water temperature, as demonstrated here. Application of a well-controlled current supply algorithm or waveform, rather than a constant current approach, could benefit an electrolyser in gaining overall energy efficiency.
- The dynamic heat balance hypothesis proposed here explains qualitatively the results obtained above. However, a computational model is needed to confirm and quantify the hypothesis, as well as to extend the results to practical and more complex stack configurations. This is the subject of another paper.
- At high current, a sharp increase in the operating current can lead to a significant overshoot of stack voltage, representing high energy consumption. Therefore, for the PEMWE stack, a slow ramping-up of current is preferred in order to save energy. A slow ramp up in current seems not to be detrimental to cell voltage,[32] and hence not to efficiency. Since continuously increasing current will also cause elevated voltage and temperature, a start-up procedure incorporating current modulation should be considered to obtain optimum performance.

With an urgency to store renewable-energy-sourced electricity in green H_2 to meet the net zero carbon emission, its intermittent nature can challenge large-scale water electrolyser efficiency. A corresponding electrolyser control algorithm, such as the operating current waveform and thermal management, should be considered to obtain the optimum operating performance. Understanding the interaction between current dynamics and cell thermal/electrical performance in both transient and steady states, and control regime of the current dynamic will mitigate the voltage aging/degrading in a water electrolyser. While our experiments can represent single cell and small stacks, different behaviour could be expected with larger stacks, as thermal and kinetic flow dynamics will affect the system's response to transient operating current variation. However, our research showed evidence the improvement of energy efficiency was higher in the 2-cell stack than the 1 cell stack.

Acknowledgments

We acknowledge the New Zealand Product Accelerator (CFX05059) to fund this project. This work is also supported by the Marsden Fund Council, administered by the Royal Society of New Zealand (MFP-UOA2111). We truly appreciate the laboratory support from our technician David Cotton, and the discussion with Dr Seho Kim and Dr Andrea Kolb from the University of Auckland.

ORCID

Jingjing Liu https://orcid.org/0000-0002-1985-5397

References

1. A. Brown, "'Uses of hydrogen: I. Industry." *The Chemical Engineering*, **2019**(July/Aug), 41 937/938 (2019).
2. A. Buttler and H. Spliethoff, "Current status of water electrolysis for energy storage, grid balancing and sector coupling via power-to-gas and power-to-liquids: a review." *Renew. Sustain. Energy Rev.*, **82**, 2440 (2018).
3. T. Smolinka, E. T. Ojong, and J. Garche, "Chapter 8 Hydrogen production from renewable energies—electrolyzer technologies." (2015), in*Electrochemical Energy Storage for Renewable Sources and Grid Balancing* (Elsevier, Amsterdam) 103.
4. IEA, *The Future of Hydrogen - Seizing Today's Opportunities* (International Energy Agency, Paris) (2019).
5. S. Sharma and S. K. Ghoshal, "Hydrogen the future transportation fuel: from production to applications." *Renew. Sustain. Energy Rev.*, **43**, 1151 (2015).
6. P. Millet, R. Ngameni, S. Grigoriev, and V. Fateev, "Scientific and engineering issues related to PEM technology: Water electrolysers, fuel cells and unitized regenerative systems." *Int. J. Hydrogen Energy*, **36**, 4156 (2011).
7. Z. Dobó and Á. B. Palotás, "Impact of the current fluctuation on the efficiency of Alkaline Water Electrolysis." *Int. J. Hydrogen Energy*, **42**, 5649 (2017).
8. C. Lamy and P. Millet, "A critical review on the definitions used to calculate the energy efficiency coefficients of water electrolysis cells working under near ambient temperature conditions." *J. Power Sources*, **447**, 1 (2020).
9. J. Liu, J. Kennedy, A. T. Marshall, J. Metson, and M. Taylor, "'Challenges in green hydrogen production with renewable and varying electricity supply: an electrochemical engineering perspective,." *J. Electrochem. Soc.*, **169**, 1 (2022), Art no. 114503.
10. M. Mori, T. Mrzljak, B. Drobnič, and M. Sekavčnik, "Integral characteristics of hydrogen production in alkaline electrolysers." *Strojniški Vestnik-Journal of Mechanical Engineering*, **59**, 585 (2013).
11. F.-W. Speckmann, S. Bintz, and K. P. Birke, "Influence of rectifiers on the energy demand and gas quality of alkaline electrolysis systems in dynamic operation." *Appl. Energy*, **250**, 855 (2019).
12. A. Bergen, L. Pitt, A. Rowe, P. Wild, and N. Djilali, "Transient electrolyser response in a renewable-regenerative energy system." *Int. J. Hydrogen Energy*, **34**, 64 (2009).
13. F. Rocha, Q. de Radiguès, G. Thunis, and J. Proost, "Pulsed water electrolysis: a review." *Electrochim. Acta*, **377**, 1 (2021).
14. P. Lavoie, S. Namboothiri, M. Dorreen, J. J. Chen, D. P. Zeigler, and M. P. Taylor, "Increasing the power modulation window of aluminium smelter pots with shell heat exchanger technology." *Light Metals* , **2011**, 367 (2011).
15. M. P. Taylor and J. J. Chen, "Technique for low amperage potline operation for electricity grid storage." *Metallurgical and Materials Transactions E*, **2**, 87 (2015).
16. J. O.-M. Bockris, I. A. Ammar, and A. K.-M. S. Huq, "The mechanism of the hydrogen evolution reaction on platinum, silver and tungsten surfaces in acid solutions." *J. Phys. Chem.*, **61**, 879 (1957).
17. M. Vanags, J. Kleperis, and G. Bajars, "Electrolyses model development for metal/electrolyte interface: testing with microrespiration sensors." *Int. J. Hydrogen Energy*, **36**, 1316 (2011).
18. J. Ghoroghchian and J. O.-M. Bockris, "Use of a homopolar generator in hydrogen production from water." *Int. J. Hydrogen Energy*, **10**, 101 (1985).
19. J. Koponen, V. Ruuskanen, A. Kosonen, M. Niemelä, and J. Ahola, "Effect of converter topology on the specific energy consumption of alkaline water electrolyzers." *IEEE Trans. Power Electron.*, **34**, 6171 (2018).
20. Q. De Radigues, G. Thunis, and J. Proost, "On the use of 3-D electrodes and pulsed voltage for the process intensification of alkaline water electrolysis." *Int. J. Hydrogen Energy*, **44**, 29432 (2019).
21. F. Rocha and J. Proost, "Discriminating between the effect of pulse width and duty cycle on the hydrogen generation performance of 3-D electrodes during pulsed water electrolysis." *Int. J. Hydrogen Energy*, **46**, 28925 (2021).
22. M. Carmo, D. L. Fritz, J. Mergel, and D. Stolten, "A comprehensive review on PEM water electrolysis." *Int. J. Hydrogen Energy*, **38**, 4901 (2013).
23. S. S. Kumar and V. Himabindu, "Hydrogen production by PEM water electrolysis–A review." *Materials Science for Energy Technologies*, **2**, 442 (2019).
24. P. Millet, A. Ranjbari, F. De Guglielmo, S. Grigoriev, and F. Auprêtre, "Cell failure mechanisms in PEM water electrolyzers." *Int. J. Hydrogen Energy*, **37**, 17478 (2012).
25. P. Millet, N. Mbemba, S. Grigoriev, V. Fateev, A. Aukauloo, and C. Etiévant, "Electrochemical performances of PEM water electrolysis cells and perspectives." *Int. J. Hydrogen Energy*, **36**, 4134 (2011).
26. C. Rakousky, G. P. Keeley, K. Wippermann, M. Carmo, and D. Stolten, "The stability challenge on the pathway to high-current-density polymer electrolyte membrane water electrolyzers." *Electrochim. Acta*, **278**, 324 (2018).
27. S. Siracusano, S. Trocino, N. Briguglio, F. Pantò, and A. S. Aricò, "Analysis of performance degradation during steady-state and load-thermal cycles of proton exchange membrane water electrolysis cells." *J. Power Sources*, **468**, 228390 (2020).
28. C. Rakousky et al., "Polymer electrolyte membrane water electrolysis: Restraining degradation in the presence of fluctuating power." *J. Power Sources*, **342**, 38 (2017).
29. F. Parache et al., "Impact of power converter current ripple on the degradation of PEM electrolyzer performances." *Membranes*, **12**, 109 (2022).
30. S. Boulevard, J. Kadjo, A. Thomas, B. G. Perez, and S. Martemianov, "Characterization of aging effects during PEM electrolyzer operation using voltage instabilities evolution." *Russ. J. Electrochem.*, **58**, 258 (2022).
31. A. H. Shaaban, "Water electrolysis and pulsed direct current." *J. Electrochem. Soc.*, **140**, 2863 (1993).
32. M. Espinosa-López et al., "Modelling and experimental validation of a 46 kW PEM high pressure water electrolyzer." *Renewable Energy*, **119**, 160 (2018).
33. M. Lebbal and S. Lecœuche, "Identification and monitoring of a PEM electrolyser based on dynamical modelling." *Int. J. Hydrogen Energy*, **34**, 5992 (2009).
34. Á. Hernández-Gómez, V. Ramirez, D. Guilbert, and B. Saldivar, "Development of an adaptive static-dynamic electrical model based on input electrical energy for PEM water electrolysis." *Int. J. Hydrogen Energy*, **45**, 18817 (2020).
35. Á. Hernández-Gómez, V. Ramirez, D. Guilbert, and B. Saldivar, "Cell voltage static-dynamic modeling of a PEM electrolyzer based on adaptive parameters: development and experimental validation." *Renewable Energy*, **163**, 1508 (2021).
36. R. García-Valverde, N. Espinosa, and A. Urbina, "Simple PEM water electrolyser model and experimental validation." *Int. J. Hydrogen Energy*, **37**, 1927 (2012).
37. P. Atkins, J. D. Paula, and J. Keeler, "Chemical equilibrium." (2018), in*Atkins' Physical Chemistry.* (Oxford University Press, Oxford) 206.
38. E. Gileadi, *Physical Electrochemistry.* (Wiley-VCH Verlag GmbH & Co. KGaA, Weiheim) (2011).
39. P. Atkins, J. D. Paula, and J. Keeler, "Processes at solid surfaces." (2018) *Atkins' Physical Chemistry.* (Oxford University Press, Oxford) 824.
40. P. Atkins, J. Paula, and J. Keeler, "Reaction dynamics." (2018), in*Atkins' Physical Chemistry.* (Oxford University Press, Oxford)642.
41. L. F.-L. Oliveira, S. Laref, E. Mayousse, C. Jallut, and A. A. Franco, "A multiscale physical model for the transient analysis of PEM water electrolyzer anodes." *Phys. Chem. Chem. Phys.*, **14**, 10215 (2012).
42. P. Atkins, J. D. Paula, and K. J, "Solids." (2018) *Atkins' Physical Chemistry* (Oxford University Press, Oxford) 642.
43. W. Wang, X. Wei, D. Choi, X. Lu, G. Yang, and C. Sun, "Electrochemical cells for medium-and large-scale energy storage: fundamentals." *Advances in Batteries for Medium and Large-Scale Energy Storage* (Elsevier, Amsterdam)3 (2015), in .
44. P. Millet et al., "PEM water electrolyzers: from electrocatalysis to stack development." *Int. J. Hydrogen Energy*, **35**, 5043 (2010).
45. Á. Hernández-Gómez, V. Ramirez, and D. Guilbert, "Investigation of PEM electrolyzer modeling: electrical domain, efficiency, and specific energy consumption." *Int. J. Hydrogen Energy*, **45**, 14625 (2020).
46. A. Aricò, S. Siracusano, N. Briguglio, V. Baglio, A. Di Blasi, and V. Antonucci, "Polymer electrolyte membrane water electrolysis: status of technologies and potential applications in combination with renewable power sources." *J. Appl. Electrochem.*, **43**, 107 (2013).
47. G. Papakonstantinou, G. Algara-Siller, D. Teschner, T. Vidaković-Koch, R. Schlögl, and K. Sundmacher, "Degradation study of a proton exchange membrane water electrolyzer under dynamic operation conditions." *Appl. Energy*, **280**, 115911 (2020).
48. U. Babic, M. Suermann, F. N. Büchi, L. Gubler, and T. J. Schmidt, "Critical review—identifying critical gaps for polymer electrolyte water electrolysis development." *J. Electrochem. Soc.*, **164**, F387 (2017).
49. Q. Feng, G. Liu, B. Wei, Z. Zhang, H. Li, and H. Wang, "A review of proton exchange membrane water electrolysis on degradation mechanisms and mitigation strategies." *J. Power Sources*, **366**, 33 (2017).
50. S. H. Frensch, F. Fouda-Onana, G. Serre, D. Thoby, S. S. Araya, and S. K. Kær, "Influence of the operation mode on PEM water electrolysis degradation." *Int. J. Hydrogen Energy*, **44**, 29889 (2019).
51. A. Villagra and P. Millet, "An analysis of PEM water electrolysis cells operating at elevated current densities." *Int. J. Hydrogen Energy*, **44**, 9708 (2019).
52. M. Möckl, M. Bernt, J. Schröter, and A. Jossen, "Proton exchange membrane water electrolysis at high current densities: Investigation of thermal limitations." *Int. J. Hydrogen Energy*, **45**, 1417 (2020).
53. J. Mališ, P. Mazúr, M. Paidar, T. Bystron, and K. Bouzek, "Nafion 117 stability under conditions of PEM water electrolysis at elevated temperature and pressure." *Int. J. Hydrogen Energy*, **41**, 2177 (2016).
54. Z. Ma, L. Witteman, J. A. Wrubel, and G. Bender, "A comprehensive modeling method for proton exchange membrane electrolyzer development." *International Journal of Hydrogen Energy*, **28**, 1141 (2021).
55. K. Qian, J. J. Chen, and N. Matheou, "Visual observation of bubbles at horizontal electrodes and resistance measurements on vertical electrodes." *J. Appl. Electrochem.*, **27**, 434 (1997).
56. K. Qian, Z. Chen, and J. Chen, "Bubble coverage and bubble resistance using cells with horizontal electrode." *J. Appl. Electrochem.*, **28**, 1141 (1998).
57. S. Mazloomi and N. Sulaiman, "Influencing factors of water electrolysis electrical efficiency." *Renew. Sustain. Energy Rev.*, **16**, 4257 (2012).
58. L. Huang, "The energy analysis of a Proton Exchange Membrane (PEM) electrolyser cell under fluctuating current density." *Masters Eng* (Chemical and Materials Eng, University of Auckland, Auckland, New Zealand) (2022), [Online]. Available: https://hdl.handle.net/2292/60414.
59. D. T. Filip Smeets, "HyBALANCE: state of the art PEM electrolysis paving the way to multi-MW renewable hydrogen systems." *Hydrogenics Europe N.V.* (HyBalance Inauguration Ceremony, Oevel Belgium) (2017), [Online]. Available: http://hybalance.eu/wp-content/uploads/2016/03/Hydrogenics-presentation_HyBalance-inauguration.pdf.